Biochemical Pharmacology 89 (2014) 52–61

Contents lists available at ScienceDirect

Biochemical Pharmacology

journal homepage: www.elsevier.com/locate/biochempharm

# Telatinib reverses chemotherapeutic multidrug resistance mediated by ABCG2 efflux transporter *in vitro* and *in vivo*

Kamlesh Sodani [a,1], Atish Patel [a], Nagaraju Anreddy [a], Satyakam Singh [a], Dong-Hua Yang [b], Rishil J. Kathawala [a], Priyank Kumar [a], Tanaji T. Talele [a], Zhe-Sheng Chen [a,*]

[a] Department of Pharmaceutical Sciences, College of Pharmacy and Health Sciences, St. John's University, Queens, NY 11439, USA
[b] Biosample Repository Facility, Fox Chase Cancer Center, Philadelphia, PA 19111, USA

ARTICLE INFO

*Article history:*
Received 8 November 2013
Accepted 12 February 2014
Available online 22 February 2014

*Keywords:*
ABC transporter
ABCG2
Multidrug resistance
Telatinib
Tyrosine kinase inhibitor

ABSTRACT

Multidrug resistance (MDR) is a phenomenon where cancer cells become simultaneously resistant to anticancer drugs with different structures and mechanisms of action. MDR has been shown to be associated with overexpression of ATP-binding cassette (ABC) transporters. Here, we report that telatinib, a small molecule tyrosine kinase inhibitor, enhances the anticancer activity of ABCG2 substrate anticancer drugs by inhibiting ABCG2 efflux transporter activity. Co-incubation of ABCG2-overexpressing drug resistant cell lines with telatinib and ABCG2 substrate anticancer drugs significantly reduced cellular viability, whereas telatinib alone did not significantly affect drug sensitive and drug resistant cell lines. Telatinib at 1 μM did not significantly alter the expression of ABCG2 in ABCG2-overexpressing cell lines. Telatinib at 1 μM significantly enhanced the intracellular accumulation of [$^3$H]-mitoxantrone (MX) in ABCG2-overexpressing cell lines. In addition, telatinib at 1 μM significantly reduced the rate of [$^3$H]-MX efflux from ABCG2-overexpressing cells. Furthermore, telatinib significantly inhibited ABCG2-mediated transport of [$^3$H]-$E_2$17βG in ABCG2 overexpressing membrane vesicles. Telatinib stimulated the ATPase activity of ABCG2 in a concentration-dependent manner, indicating that telatinib might be a substrate of ABCG2. Binding interactions of telatinib were found to be in transmembrane region of homology modeled human ABCG2. In addition, telatinib (15 mg/kg) with doxorubicin (1.8 mg/kg) significantly decreased the growth rate and tumor size of ABCG2 overexpressing tumors in a xenograft nude mouse model. These results, provided that they can be translated to humans, suggesting that telatinib, in combination with specific ABCG2 substrate drugs may be useful in treating tumors that overexpress ABCG2.



## 1. Introduction

Multidrug resistance (MDR) is a phenomenon of simultaneous resistance exhibited by cancer cells to anticancer drugs with different structures and mechanisms of action [1,2]. MDR is often associated with overexpression of transmembrane ATP-binding cassette (ABC) transporters [2]. ABC transporter-subfamily B member 1 (ABCB1/P-gp/MDR1), ABC transporter-subfamily C member 1 (ABCC1/MRP1) and ABC transporter-subfamily G member 2 (ABCG2/BCRP/MXR/ABCP) are the major ABC transporters that have been implicated in the development of MDR [3–5]. These ABC transporters reduce the amount of anticancer drug inside cancer cells by eliminating substrate anticancer drugs against the concentration gradient by ATP-dependent active efflux [1,3,5,6]. It leads to intracellular levels of anticancer drugs below the cytotoxic effect and renders the cancer cells mostly unaffected.

ABCG2 is localized apically in polarized cells, such as blood–brain barrier and intestinal enterocytes, where it can influence the oral absorption and pharmacokinetics of several anticancer drugs [7,8]. Human ABCG2 has a broad substrate profile that includes several anticancer drugs, ranging from organic anion conjugates, nucleoside analogs, organic dyes, and tyrosine kinase inhibitors (TKIs) to anthracyclines [9,10]. Although evidence of ABCG2 involvement in clinical MDR is accumulating, there is no lack of conflicting results between ABCG2 expression and drug response [11,12]. Some studies have reported association between ABCG2 expression and poor chemotherapeutic response. Increased *ABCG2*

*Abbreviations:* ABC, ATP-binding cassette; ABCB1, ABC transporter-subfamily B member 1; ABCG2, ABC transporter-subfamily G member 2; MDR, multidrug resistance; VEGFR, vascular endothelial growth factor receptor; TKI, tyrosine kinase inhibitor.

* Corresponding author.
*E-mail address:* chenz@stjohns.edu (Z.-S. Chen).
[1] Current address: Oncology and Cell Biology Center, The Feinstein Institute for Medical Research, Manhasset, NY 11030, USA.

http://dx.doi.org/10.1016/j.bcp.2014.02.012
0006-2952/

gene expression has also been associated with poor response to chemotherapy in childhood acute myeloid leukemia (AML) and relapsed AML [13,14]. In addition, increased ABCG2 mRNA has been reported in irinotecan treated hepatic metastases than in irinotecan-naive metastases [15]. ABCG2 expression has been reported in various solid tumors, such as digestive tract, endometrium and melanoma [16]. ABCG2 expression has also been reported in leukemia, especially in pediatric AML [17]. ABCG2 is also reported as a molecular marker for side-population (SP) characterization [18]. SP cells are isolated from various solid and hematological malignancies [19–22]. These SP cells were shown to have cells with stem cell-like properties, such as self-renewal and resistance to anticancer drugs [20,22–24]. These cancer stem cells with drug resistance capability are thought to be responsible for the tumor regrowth and ABCG2 is most likely an efflux transporter providing a protective mechanism against anticancer drugs [24]. It suggests that inhibition of the efflux function of the ABCG2 transporter can enhance the cytotoxic effects of anticancer drugs.

Enormous efforts have been devoted toward discovery and development of ABCB1 inhibitors [10]. However, none of the clinical trials with ABCB1 inhibitors have been clinically successful [10]. In addition, very little efforts have been devoted toward studies concerning ABCG2 inhibitor, and few specific inhibitors have been identified. Small molecule inhibitors of ABCG2 may be useful to combat ABCG2-mediated drug resistance, to improve bioavailability of orally administered ABCG2 substrate drugs, and to kill the putative cancer stem cells with ABCG2 expression. Many compounds such as fumitremorgin C (FTC), lapatinib and its analogs, erlotinib and nilotinib have been shown to inhibit ABCG2 *in vitro* [25–30]. However, very few studies have shown the effect of selective ABCG2 inhibitors on drug resistance *in vivo*. No drug specifically inhibiting ABCG2 has been clinically approved yet. Accordingly, a specific ABCG2 inhibitor with an *in vivo* effect on MDR would be a good candidate for clinical trial.

Telatinib is a potent and orally available TKI of vascular endothelial growth factor receptor (VEGFR)-2, VEGFR-3, platelet-derived growth factor receptor-β (PDGFR-β) and cKIT (stem cell growth factor receptor) [31]. It is currently in clinical trial for gastric and colorectal cancer by ACT biotech (http://www.actbio-tech.com/pipeline.html). In addition, telatinib combination does not add toxicity when combined at monotherapy dose with chemotherapy (http://meeting.ascopubs.org/cgi/content/abstract/28/15_suppl/e14575). In the current study we have examined the effect of telatinib on ABCG2-mediated drug resistance in cancer cell lines in relation to ABCG2 expression *in vitro* and *in vivo*.

## 2. Methods and materials

### 2.1. Chemicals

[$^3$H]-mitoxantrone (MX) (4 Ci/mmol) was purchased from Moravek Biochemicals, Inc. (Brea, CA). Dulbecco's modified Eagle's medium (DMEM), fetal bovine serum (FBS), penicillin/streptomycin and trypsin 0.25% were purchased from Hyclone (Waltham, MA). The monoclonal antibodies BXP-21 (against ABCG2), sc-8432 (against actin) and the secondary horseradish peroxidase-labeled anti-mouse IgG were purchased from Santa Cruz Biotechnology, Inc. (Santa Cruz, CA). GAPDH rabbit monoclonal antibody was purchased from cell signaling (Danvers, MA). Alexa Fluor® 488 Goat Anti-Mouse antibody for immunofluorescence was purchased from Life Technologies (Grand Island, NY). Human ABCG2 (Arg482) membranes were purchased from BD Bioscience (Woburn, MA). FTC was synthesized by Thomas McCloud, Developmental Therapeutics Program, and Natural Products Extraction Laboratory, NIH (Bethesda, MD) and was a gift from Dr. Susan Bates. ONO-1078 (specific ABCC1 inhibitor) was a gift from Dr. Shin-ichi Akiyama (Kagoshima, Japan). Telatinib was purchased from Selleck chemicals (Houston, TX). Doxorubicin (DOX) was purchased from LC laboratories (Woburn, MA). MX, SN-38, verapamil, cisplatin, 3-(4,5-dimethylthiazol-yl)-2,5-diphenyl-tetrazolium bromide (MTT), dimethyl sulfoxide (DMSO) and other chemicals were obtained from Sigma Chemical Co. (St. Louis, MO).

### 2.2. Cell lines

HEK293/pcDNA3.1 (parental), ABCG2-482-R2, ABCG2-482-G2 and ABCG2-482-T7 cell lines were established by selection with G418 (2 mg/mL) after transfecting HEK293 cell line with either an empty pcDNA3.1 vector or pcDNA3.1 vector containing a full length *ABCG2* with Arg, Gly or Thr at position 482, respectively, and were cultured in a medium with 2 mg/mL of G418. The H460 (non small cell lung cancer), S1 (colorectal cancer cell line), ABCG2 overexpressing H460/MX20 and S1-M1-80 cells were kindly provided by Dr. Susan Bates and Robert Robey (NCI, NIH, Bethesda). The KB-C2 cell line overexpressing ABCB1, was established by a step-wise exposure of KB-3-1, a parental human epidermoid carcinoma cell line, to increasing concentration of colchicine up to 2 μg/mL [32]. *ABCC1*-transfected HEK/ABCC1 cells were kindly provided by Dr. Suresh Ambudkar (NCI, NIH, Bethesda, MD). All cells were grown as adherent monolayer in drug-free culture media for more than 2 weeks before assay. All cell lines were cultured at 37 °C with 5% $CO_2$ and DMEM containing 10% FBS and 1% penicillin/streptomycin.

### 2.3. Cytotoxicity determination by MTT assay

Briefly, cells were harvested and re-suspended at a final concentration of $3 \times 10^3$ cells/well for KB-3-1 and H460 cells, and $5 \times 10^3$ cells/well for KB-C2, H460/MX20, ABCG2-482-R2, S1-M1-80, HEK293/pcDNA3.1, ABCG2-482-G2, ABCG2-482-T7 and HEK/ABCC1 cells. Cells were seeded evenly into (160 μl/well) 96-well plate. After incubating for 24 h at 37 °C, 20 μl of different concentrations of the anticancer drug (prepared in PBS with final DMSO concentration of 0.01%) were added (20 μl of a fixed concentration of the inhibitor was added 1 h prior to the addition of anticancer drug). Subsequently the cells were incubated at 37 °C for 72 h. After 72 h, 20 μl MTT (4 mg/ml) was added to each well. The plates were incubated at 37 °C for 4 h. The MTT was gently aspirated from each well without disturbing the cells, and 100 μl of DMSO was added to dissolve the purple formazan crystals. Finally, the absorbance was read at 570 nm with the help of Opsys microplate reader (Dynex Technologies, Chantilly, VA). The $IC_{50}$ was calculated in accordance with the bliss method [33].

### 2.4. [$^3$H]-MX accumulation and efflux assay

The parental HEK293/pcDNA3.1, ABCG2-482-R2, ABCG2-482-G2 and ABCG2-482-T7 cells were trypsinized and two aliquots ($12 \times 10^6$ cells) from each cell line were suspended in the medium, pre-incubated with or without reversal agent (Telatinib or FTC) at 37 °C for 1 h. Subsequently, cells were suspended in the medium containing 0.1 μM [$^3$H]-MX with or without the reversal compound at 37 °C for 2 h. The cells were washed with cold phosphate-buffered saline (PBS) for three times and radioactivity was measured. Briefly, parental HEK293-pcDNA3.1 and ABCG2-482-R2 cells were trypsinized and two aliquots ($48 \times 10^6$ cells) from each cell line were suspended in the medium, pre-incubated with or without reversal agent at 37 °C for 1 h. Subsequently, cells were suspended in the medium containing 0.1 μM [$^3$H]-MX with or without reversal agent at 37 °C for 2 h. The cells were washed with cold PBS for three times, and then suspended in fresh medium with or without telatinib at 37 °C. Aliquots ($1 \times 10^6$ cells) were collected

at various time points (0, 60, 120, and 240 min). Radioactivity was measured in a Packard TRI-CARB® 1900CA liquid scintillation analyzer from Packard Instrument Company, Inc. (Downers Grove, IL).

### 2.5. Western blot analysis

Cell lysates from H460/MX20 cell line were prepared as described previously. Equal amounts of total cell lysates (30 μg protein) were resolved by sodium dodecyl sulfate polyacrylamide gel electrophoresis (SDS-PAGE) and electrophoretically transferred onto polyvinylidene fluoride (PVDF) membranes. After incubation in a blocking solution in TBST buffer (10 mM Tris–HCl, pH 8.0, 150 mM NaCl, and 1% Tween 20) for 1 h at room temperature, the membranes were incubated overnight with primary monoclonal antibodies against either actin/GAPDH at 1:1000 dilution or ABCG2 at 1:200 dilution at 4 °C, and were then further incubated for 2 h at room temperature with horseradish peroxide (HRP)-conjugated secondary antibody (1:1000 dilution). The protein–antibody complex was detected by enhanced chemiluminescence detection system (Amersham, NJ).

### 2.6. Immunocytochemistry analysis

For immunocytochemistry analysis, H460 and H460/MX20 cells ($0.5 \times 10^3$) were seeded in 24 well plates. Cells were incubated with or without telatinib (1 μM) for 72 h. Thereafter, cells were washed with PBS and fixed with 4% paraformaldehyde for 15 min at room temperature and then rinsed with PBS three times. Followed by permeabilization with 1% triton X-100 for 10 min at 4 °C. Cells were again washed for three times with PBS. Then cells were blocked with 2 mg/ml of BSA for 1 h at 37 °C. Fixed cells were incubated with monoclonal antibody against ABCG2 (BXP 21) (1:50) for 1 h at 37 °C, followed by three washes with PBS. Then cells were further incubated with Alexa flour 488 goat anti-mouse IgG (1:60) for 1 h at 37 °C. DAPI was used for nuclear counter-staining. Immunofluorescence images were taken with a fluorescence microscope (Nikon eclipse TE2000-S, Melville, NY).

### 2.7. ATPase assay of ABCG2

The vanadate (Vi)-sensitive ATPase activity of ABCG2 in the membrane of High Five insect cells was measured as per supplier's instructions and previously described. Briefly, membrane (2 μg/0.06 ml) were incubated in ATPase assay buffer (50 mM MES, pH 6.8, 50 mM KCl, 5 mM sodium azide, 2 mM EGTA, 2 mM dithiothreitol, 1 mM ouabain, and 10 mM $MgCl_2$) with or without 0.4 mM vanadate at 37 °C for 5 min and then incubated with varying concentrations of telatinib at 37 °C for 5 min. The ATPase reaction was started by the addition of 4 mM Mg-ATP. After incubating at 37 °C for 10 min, the reactions were stopped by adding 0.05 mL of 10% SDS solution. The liberated inorganic phosphate was measured as previously described [34].

### 2.8. Inside-out vesicle uptake assay

For the uptake assay, we used HEK293/pcDNA3.1 and ABCG2 overexpressing ABCG2-482-R2 cell membrane vesicles. The experiment was carried out using a rapid filtration method, as previously described [35] in a medium containing membrane vesicles (10 μg), 0.25 M sucrose, 10 mM Tris–HCl, pH 7.4, 10 mM $MgCl_2$, 4 mM AMP/ATP, 10 mM phosphocreatine, 100 μg/ml creatine phosphokinase, and radio labeled substrate ([$^3$H]-$E_2$17βG) with unlabeled substrate, in a total volume of 50 μl. Reactions were carried out at 37 °C for 10 min and was stopped by adding 3 ml of an ice-cold stop solution (0.25 M sucrose, 100 mM NaCl, 10 mM Tris–HCl, pH 7.4). Samples were passed through 0.22 μM Dura pore membrane filters (Millipore, Bedford, MA) under vacuum. The filters were washed three times with 3 ml of ice-cold stop solution and dried at room temperature for 30 min. Radioactivity was measured by the use of a liquid scintillation counter. The rates of net ATP-dependent transport were determined by subtracting the values obtained in the presence of 4 mM AMP from those obtained in the presence of 4 mM ATP.

### 2.9. Molecular modeling – ABCG2

#### 2.9.1. Ligand structure preparation

Telatinib structure was built using the fragment dictionary of Maestro v9.0 and energy minimized by Macromodel program v9.7 (Schrödinger, Inc., New York, NY, 2009). The low-energy 3D structures of telatinib were generated by LigPrep v2.3 as described previously. Conformational search on LigPrep generated ligand structure was performed as per previous study [28].

#### 2.9.2. Protein structure preparations and docking protocol

Homology model of ABCG2 was built based on the mouse p-glycoprotein (PDB ID: 3G5U) [36] as template and has been generated and provided the to us by Rosenberg et al. [37,38]. The homology model of ABCG2 was energy minimized before initiating grid preparation. To identify the druggable sites on ABCG2 homology model, we have generated various grids based on the following residues as centroids, for example, Arg482 (grid 1), Asn629 (grid 2), Arg383 (grid 3) and Leu241 along with Gly83 (grid 4). The choices of these residues were based on their involvement in ABCG2 function as determined through mutational experiments [39–42]. The grid 1 generated using Arg482 as the centroid was found to have the best docking score; hence the docking discussion is based on binding mode of the top scoring telatinib conformation at the site of Arg482 generated grid 1. Glide v5.0 docking protocol was followed with the default functions (Schrödinger, Inc., New York, NY, 2009). All computations were carried out on a Dell Precision 470n dual processor with the Linux OS (Red Hat Enterprise WS 4.0).

### 2.10. Animals

Male athymic NCR (nu/nu) nude mice (13–15 g, aged 4–5 weeks), were purchased from the Taconic Farms (NCRNU-M, Homozygous, Albany, NY) and were used for tumor xenograft. All the animals were maintained on an alternating 12 h light/dark cycle with free access to water and rodent chow ad libitum. The mice were maintained at the St. John's University Animal Facility and were monitored closely for tumor growth by palpation and visual examination. Institutional Animal Care & Use Committee (IACUC) of St. John's University approved this project, and the research was conducted in compliance with the Animal Welfare Act and other federal statutes.

### 2.11. Nude mice ABCG2-overexpressing tumor xenograft model

Briefly, H460 ($1 \times 10^6$) and H460/MX20 ($3 \times 10^6$) cells were injected s.c. under the armpits. Tumors that fail to reach a volume of 30 mm$^3$ at the start of treatment were not used in this study. The mice were randomized into four groups ($n = 8$) and treated with one of the following regimens: (a) vehicle (10% N-methyl-pyrrolidinone, 90% polyethylene glycol 300) (q3d × 6), (b) DOX (1.8 mg/kg, i.p., q3d × 6), (c) telatinib dissolved in 10% N-methyl-pyrrolidinone, 90% polyethylene glycol 300 (15 mg/kg, p.o., every 2nd and 3rd day; total 12 times), and (d) DOX (1.8 mg/kg, i.p., q3d × 6) + telatinib (15 mg/kg, p.o., every 2nd and 3rd day, given 1 h before giving DOX; total 12 times). DOX for injection was prepared by dissolving in saline. Tumor volume was measured using

calipers and body weights were recorded. The two perpendicular diameters of tumors (termed A and B) were recorded every 3rd day and tumor volume (V) was estimated according to the formula published previously [30]. At the end of the study, animals were euthanized by carbon dioxide, tumor tissue were excised and fixed in 10% formalin for immunohistochemistry.

### 2.12. Immunohistochemistry

Tumors were collected, fixed in 10% neutral buffered formalin (NBF) and embedded in paraffin. Sections were cut at 5-μm, deparaffinized by xylene and rehydrated in decreasing concentration of ethanol. Boiling sections on 10 mM citrate buffer for 20 min achieved antigen retrieval. After blocking of endogenous peroxidase with 3% hydrogen peroxidase in methanol, non-specific reaction was blocked with 1% BSA at room temperature for 30 min. The sections were next incubated with the primary antibody against ABCG2 at the dilution of 1:100, at 4 °C overnight. After washing in TBS for three times, sections were incubated with labeled polymer-HRP anti-mouse (DAKO) secondary antibody at room temperature for 1 h. The sections were then exposed to DAB (diaminobenzidine tetrahydrochloride) solution and counter-stained with hematoxylin. Finally sections were dehydrated in increasing concentration of ethanol, cleared in xylene and mounted in Permount. Images were taken by Nikon Eclipse E600 microscope using NIS Elements D3.0 software.

### 2.13. Statistical analysis

Differences of the parameters between two groups were analyzed by two-tailed Student's $t$ test. $P < 0.05$ was considered as statistically significant.

## 3. Results

### 3.1. Telatinib significantly potentiates the cytotoxicity of ABCG2 substrate anticancer drugs, but not those for ABCB1 and ABCC1

Cytotoxicity of telatinib alone on ABCG2-overexpressing cell lines was analyzed and was found to be nontoxic with $IC_{50}$ values of more than 10 μM (data not shown). Subsequently, a concentration range of 0.25, 0.5 and 1 μM, was selected at which the ABCG2 inhibition ability of telatinib was analyzed for further experiments. HEK293 cells transfected with wild-type (ABCG2-482-R2) and mutant (ABCG2-482-G2 and ABCG2-482-T7) *ABCG2* showed significant resistance to MX and SN-38 (an active metabolite of topotecan) compared to HEK293/pcDNA3.1. Telatinib significantly potentiated the cytotoxicity of MX and SN-38 in *ABCG2*-transfected cell lines in a concentration dependent manner (Table 1). In addition, the reversal effect of telatinib on ABCG2-mediated MDR was comparable to the effect produced by 2.5 μM of FTC, a known ABCG2 inhibitor (Table 1). However, telatinib did not sensitize *ABCG2*-transfected cells to cisplatin, a nonsubstrate of ABCG2 (Table 1). In addition, the reversal effect of telatinib was also analyzed in parental H460 and S1, drug selected ABCG2 overexpressing H460/MX20 and S1-M1-80 cells. We found similar results where telatinib significantly increased the cytotoxicity of MX and DOX in ABCG2 overexpressing H460/MX20 and S1-M1-80 cells, respectively (Table 1). However, telatinib did not sensitize the parental HEK293/pcDNA3.1, H460 and S1 cells to ABCG2 substrate anticancer drugs (Table 1). Separately, the effect of telatinib on ABCB1- and ABCC1-mediated MDR was also analyzed. We found that telatinib did not affect the ABCB1- and ABCC1-mediated MDR in ABCB1 overexpressing KB-C2 cells and ABCC1 overexpressing HEK/ABCC1 cell, respectively (data not shown).

**Table 1**
Telatinib effectively sensitizes ABCG2 overexpressing cells to the substrate anticancer drugs.

| Treatments | $IC_{50} \pm SD$ (nM) | | | | | | | |
|---|---|---|---|---|---|---|---|---|
| | HEK293/pcDNA3.1 | RF | ABCG2-482-R2 | RF | ABCG2-482-G2 | RF | ABCG2-482-T7 | RF |
| Mitoxantrone | 48.7 ± 6.9 | 1.0 | 451.8 ± 86.8 | 9.3 | 865.4 ± 105.7 | 17.8 | 565.4 ± 75.7 | 11.6 |
| +Telatinib – 0.25 μM | 48.6 ± 5.2 | 1.0 | 263.3 ± 33.7* | 5.4 | 418.2 ± 39.6* | 8.6 | 318.2 ± 43.6* | 6.5 |
| +Telatinib – 0.5 μM | 45.9 ± 4.9 | 0.9 | 174.8 ± 28.2* | 3.6 | 275.5 ± 18.9* | 5.6 | 145.5 ± 18.9* | 3.0 |
| +Telatinib – 1 μM | 46.8 ± 7.3 | 1.0 | 66.5 ± 10.4* | 1.4 | 75.4 ± 15.4* | 1.5 | 55.4 ± 5.4* | 1.1 |
| +FTC – 2.5 μM | 44.2 ± 4.7 | 0.9 | 64.1 ± 9.5* | 1.3 | 68.4 ± 5.4* | 1.4 | 53.4 ± 3.4* | 1.1 |
| SN-38 | 11.2 ± 2.9 | 1.0 | 297.9 ± 45.6 | 26.6 | 234.2 ± 15.6 | 20.9 | 192.2 ± 29.6 | 17.1 |
| +Telatinib – 0.25 μM | 13.5 ± 3.6 | 1.2 | 192.3 ± 29.8* | 17.2 | 141.4 ± 22.6* | 12.6 | 147.7 ± 15.6* | 13.2 |
| +Telatinib – 0.5 μM | 12.8 ± 3.3 | 1.1 | 115.8 ± 19.3* | 10.3 | 83.2 ± 8.1* | 7.4 | 74.8 ± 9.1* | 6.7 |
| +Telatinib – 1 μM | 11.4 ± 3.7 | 1.0 | 17.6 ± 4.6* | 1.6 | 15.6 ± 2.8* | 1.4 | 17.4 ± 3.8* | 1.6 |
| +FTC – 2.5 μM | 13.8 ± 2.8 | 1.2 | 19.8 ± 2.5* | 1.7 | 16.9 ± 2.4* | 1.5 | 16.9 ± 1.4* | 1.5 |
| Cisplatin | 1981.4 ± 226.8 | 1.0 | 1814.1 ± 193.4 | 0.9 | 1881.6 ± 126.3 | 1.0 | 1883.6 ± 246.3 | 1.0 |
| +Telatinib – 1 μM | 1917.5 ± 166.8 | 0.9 | 1711.7 ± 282.6 | 0.9 | 1941.7 ± 224.6 | 1.0 | 1941.7 ± 114.6 | 1.0 |
| +FTC – 2.5 μM | 1796.3 ± 348.8 | 0.9 | 1908.2 ± 226.8 | 1.0 | 1794.7 ± 296.3 | 0.9 | 1884.7 ± 156.3 | 1.0 |

| Treatments | H460 | RF | H460/MX20 | RF |
|---|---|---|---|---|
| Mitoxantrone | 37.9 ± 4.2 | 1.0 | 8477.8 ± 223.4 | 223.6 |
| +Telatinib – 1 μM | 36.4 ± 5.1 | 0.9 | 168.4 ± 31.2* | 4.4 |
| +FTC – 2.5 μM | 38.7 ± 5.3 | 1.1 | 140.7 ± 42.8* | 3.7 |
| Cisplatin | 849.5 ± 96.4 | 1.0 | 886.6 ± 104.8 | 1.0 |
| +Telatinib – 1 μM | 945.3 ± 69.8 | 1.1 | 934.8 ± 112.4 | 1.1 |
| +FTC – 2.5 μM | 938.1 ± 85.2 | 1.1 | 898.2 ± 81.3 | 1.1 |

| Treatments | S1 | RF | S1-M1-80 | RF |
|---|---|---|---|---|
| Doxorubicin | 125.4 ± 28.2 | 1.0 | 8938.8 ± 523.4 | 71.3 |
| +Telatinib – 1 μM | 117.4 ± 44.1 | 0.9 | 564.4 ± 81.2* | 4.5 |
| +FTC – 2.5 μM | 137.7 ± 39.3 | 1.1 | 187.7 ± 28.8* | 1.5 |

Data represents the mean $IC_{50}$ values for each cell line ± SD obtained from three independent sets of experiments. The resistance fold (RF) was determined by dividing the $IC_{50}$ value of anticancer drug for HEK293/pcDNA3.1, ABCG2-482-R2, ABCG2-482-G2 and ABCG2-482-T7 in the absence or presence of reversal agents by the $IC_{50}$ value of respective anticancer drug for HEK293/pcDNA3.1 in the absence of reversal agent. Resistance fold for H460, H460/MX20, S1 and S1-M1-80 was determined in the similar fashion. FTC was used as a positive control as ABCG2 inhibitor.

* $P < 0.05$ versus the control group.

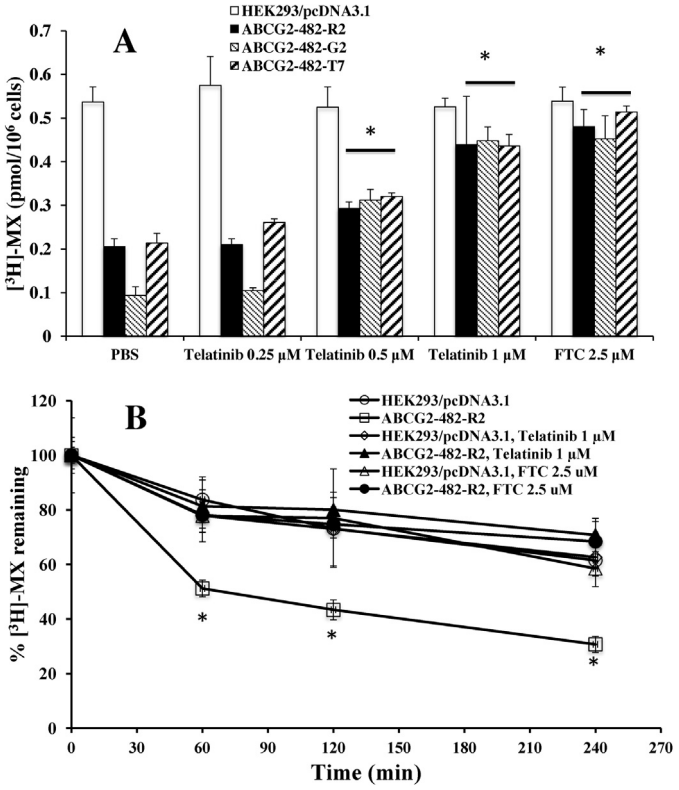


**Fig. 1.** The effect of telatinib on intracellular levels and efflux of [$^3$H]-mitoxantrone. (A) The accumulation [$^3$H]-MX in empty vector transfected HEK293/pcDNA3.1, ABCG2-482-R2, ABCG2-482-G2 and ABCG2-482-T7 cells with or without telatinib treatment. Columns are the mean of triplicate determinations. $^*P < 0.05$ versus the control group. (B) The effect of telatinib at 1 μM on retention of [$^3$H]-MX over a period of time in HEK293/pcDNA3.1 and ABCG2-482-R2. Data points represent the means ± SD. $^*P < 0.05$ versus the respective time point of control group. The figures are a representative of three independent experiments each done in triplicates.

Together these results indicate that telatinib selectively and significantly reverses the ABCG2-mediated MDR.

### 3.2. Telatinib enhances the intracellular accumulation of [$^3$H]-MX in cells overexpressing ABCG2

To explore the reversal mechanism, we examined the effect of telatinib on the intracellular accumulation of ABCG2 substrate anticancer drug in ABCG2 overexpressing cells. HEK293/pcDNA3.1 and *ABCG2*-transfected cells were incubated with [$^3$H]-MX, a known substrate of ABCG2, with or without telatinib at different concentrations for 2 h. Telatinib at 1 μM significantly increased the intracellular [$^3$H]-MX accumulation in *ABCG2*-transfected cells. However, telatinib did not significantly influence the intracellular accumulation in HEK293/pcDNA3.1 cells (Fig. 1A). These results suggest that increased intracellular levels of [$^3$H]-MX in ABCG2 overexpressing cells might be because of inhibitory effect of telatinib on drug efflux function of ABCG2 transporter.

### 3.3. Telatinib decreases the efflux of [$^3$H]-MX from cells overexpressing ABCG2

We performed a time course [$^3$H]-MX efflux analysis with or without telatinib in *ABCG2*-transfected cells to ascertain if the increase in the intracellular [$^3$H]-MX accumulation caused by telatinib was due to inhibition of [$^3$H]-MX efflux. We found that extrusion rate of [$^3$H]-MX was significantly high in ABCG2-482-R2 cells than HEK293-pcDNA3.1 cells. Telatinib at 1 μM significantly retained the intracellular [$^3$H]-MX during period of 240 min in ABCG2-482-R2. Whereas the parental cells shows no significant alterations in the intracellular levels of [$^3$H]-MX in the presence or absence of telatinib. The accumulation of [$^3$H]-MX at 60, 120 and 240 min were 51.23%, 43.37%, 30.73% with respect to the 0 min, respectively, in ABCG2-482-R2 cells in the absence of telatinib. When ABCG2-482-R2 cells were incubated with telatinib, the percentages at 60, 120 and 240 min were increased to 81.32%, 80.03% and 70.78%, respectively (Fig. 1B).

### 3.4. Telatinib does not alter the expression level of ABCG2

To analyze the effect of telatinib on the ABCG2 expression, we incubated ABCG2-482-R2 cells with telatinib at 1 μM for 24, 48 and 72 h and also at 0.25, 0.5 and 1 μM for 72 h. We found no significant decrease in the expression levels of ABCG2 upon telatinib treatment both concentration and time dependently (Fig. 2A). To evaluate if telatinib causes the translocation of ABCG2 from the plasma membrane to the cytoplasm, leading to a reduction of functional ABCG2, we performed an immunofluorescence analysis with H460 and ABCG2 overexpressing H460/MX20 cells. The results obtained showed ABCG2 expression on the membrane of H460/MX20 cells and the alteration in localization pattern is unlikely upon telatinib treatment (1 μM) for 72 h (Fig. 2B).

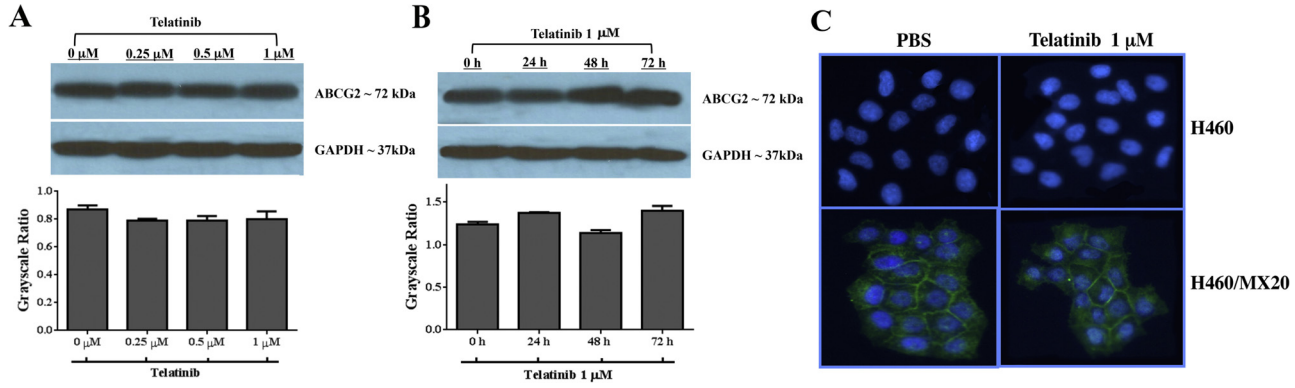


**Fig. 2.** The effect of telatinib on ABCG2 protein expression and localization. ABCG2-482-R2 cells were treated with (A) telatinib up to 1 μM for 72 h (upper panel) (B) and telatinib 1 μM over a period of 72 h (upper panel). Quantification of the obtained blots from three independent experiments is shown (lower panel). (C) The localization of ABCG2 by Immunofluorescence in H460 and H460/MX20 after treatment with telatinib 1 μM for 72 h. Immunofluorescence staining of cells with primary antibody against ABCG2 and Alexa Fluor 488-conjugated secondary antibody was observed by confocal microscope. ABCG2 specific staining is shown in green and the nuclear DNA stained by DAPI is shown in blue. Representative results are shown and similar results were obtained in two other trials. (For interpretation of the references to color in this figure legend, the reader is referred to the web version of the article.)

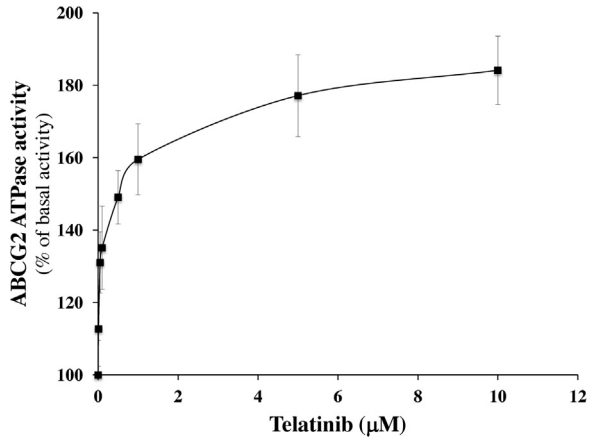


**Fig. 3.** The effect of telatinib on ATPase activity of ABCG2. The Vi-sensitive ATPase activity of ABCG2 in membrane vesicles was determined mean values are given, and the error bars represent standard error from three independent experiments.

### 3.5. Telatinib stimulates the ATPase activity of ABCG2

Several reversal agents have been reported as inhibitor and/or substrate of ABC transporters [26,27,43,44]. To determine the type of interaction of telatinib with ABCG2 ATPase, we performed an ABCG2 ATPase assay using membranes of high five insect cells overexpressing ABCG2 with different concentrations of telatinib. Telatinib stimulated the ABCG2 ATPase activity in concentration dependent manner pointing to its potential status as an ABCG2 substrate (Fig. 3).

### 3.6. Telatinib inhibits the transport of $E_2$17βG in membrane vesicles overexpressing ABCG2

With the help of inside-out membrane vesicles obtained from HEK293/-pcDNA3.1 and ABCG2-482-R2 we analyzed the ability of telatinib to inhibit the transport of the physiological substrate of wild-type ABCG2, $E_2$17βG. Here we see no change in the uptake of [$^3$H]-$E_2$17βG in the parental HEK293/pcDNA3.1 vesicles in the presence or absence of telatinib or FTC. However ABCG2-482-R2 vesicles showed increased ATP-dependent uptake of [$^3$H]-$E_2$17βG, which was effectively inhibited in the presence of telatinib at 1 μM and 2.5 μM FTC (Fig. 4). This result clearly indicates the ability of telatinib to interact with the ABCG2 membrane transporter and thereby inhibits its transport activity.

### 3.7. Docking of telatinib to human homology modeled ABCG2

The XP-Glide predicted binding mode of telatinib to human homology modeled ABCG2 [37,38] is shown in (Fig. 5). The binding energy score of telatinib with human ABCG2 was found to be −8.18 kcal/mol and shows significant interaction energy. Pyridine-2-carboxylic acid methylamide substituent of telatinib is in hydrophobic contact with Y464, S486, F489, F511, I573, P574 and L581. The carbonyl oxygen atom is involved in a hydrogen bond interaction with the side chain hydroxyl function of Y464 (–CO···OH-Y464, 2.0 Å). Moreover, the NH of the methyl amide function is involved in two electrostatic interactions, one with the oxygen atom present in side chain hydroxyl group of S486 ($CH_3NH$···OH-S486, 3.7 Å) and another with the backbone carbonyl function of I573 (–$CH_3NH$···OC-I573, 4.2 Å), which may weaken the ABCG2 activity by conformational lock. Furano-pyridazine ring was found stabilize through hydrophobic interaction with side chain of residues F507, A580, L626 and W627. Whereas the –NH linker present between the furano-pyridazine ring and chlorophenyl group is involved in electrostatic interaction

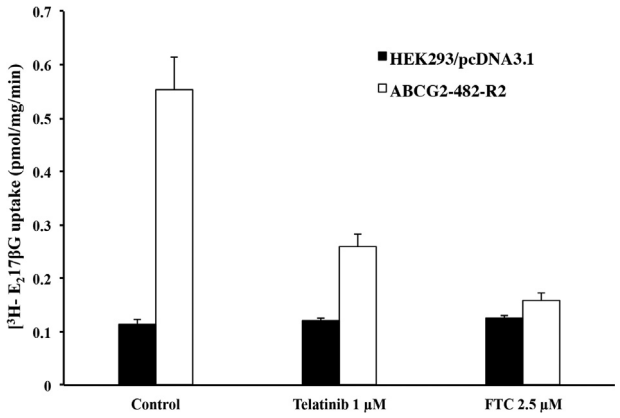


**Fig. 4.** Effect of telatinib on the ATP-dependent transport of [$^3$H]-$E_2$17βG. Membrane vesicles (10 μg) were prepared from HEK293/pcDNA3.1 and ABCG2-482-R2 cells. The rate of uptake of [$^3$H]-$E_2$17βG into membrane vesicles was measured for 10 min at 37 °C in uptake medium containing 4 mM of ATP or AMP. For inhibition experiments, membrane vesicles from HEK293/pcDNA3.1 and ABCG2-482-R2 cells were incubated with telatinib or FTC for 1 h on ice, and then transport reactions were carried out for 10 min at 37 °C in an uptake medium containing 4 mM ATP. Each column represents the mean of triplicate determinations and the bars represent SD. *$P < 0.05$, versus the control group. Experiments were repeated at least three times and a representative experiment is shown.

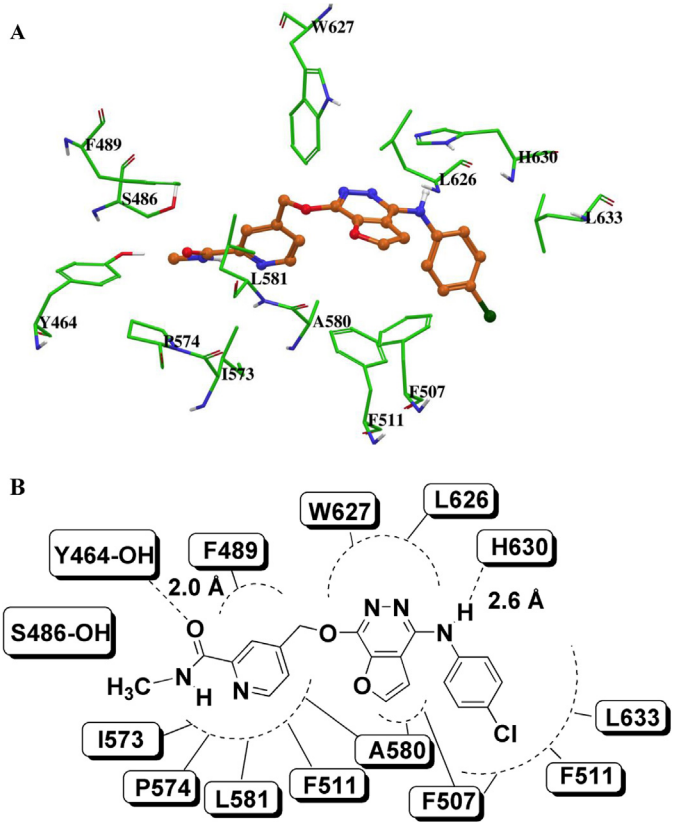


**Fig. 5.** Glide predicted binding mode of telatinib with homology modeled ABCG2. (A) The docked conformation of telatinib as ball and stick model is shown within the transmembrane region of ABCG2. Important amino acids are depicted as sticks with the atoms colored as carbon – green, hydrogen – white, nitrogen – blue and oxygen – red, whereas the telatinib is shown with the same color scheme as above except carbon atoms are represented in orange and chlorine-dark green. (B) Schematic diagram of the important interactions observed in the complex of telatinib with the binding site residues of human ABCG2. (For interpretation of the references to color in this figure legend, the reader is referred to the web version of the article.)

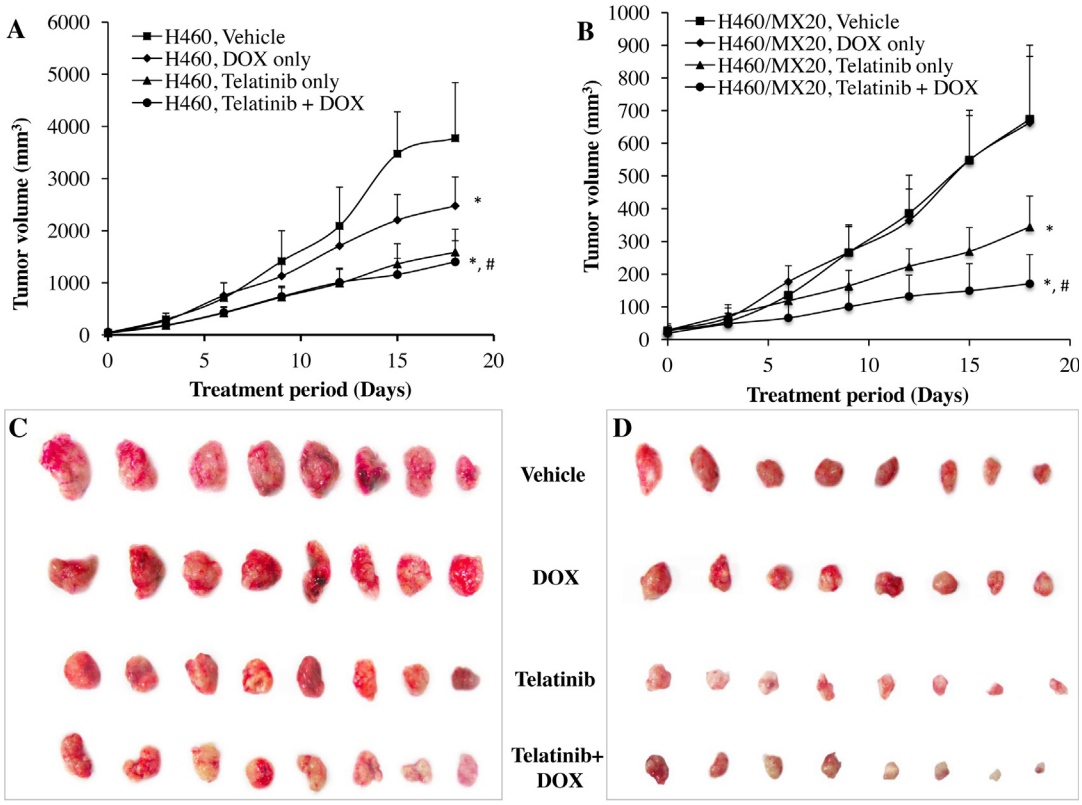


**Fig. 6.** The effect of telatinib on H460 and H460/MX20 tumor xenograft growth rate. (A) Changes in tumor volume with time in H460 xenograft are shown. (B) Changes in tumor volume with time in H460/MX20 xenograft are shown. Points represent mean tumor volume for each group after implantation. Each point on line graph represents the mean tumor volume ($mm^3$) at a particular day after implantation and the bars represent SD. (C) A representative picture of the excised H460 tumor sizes from different mice is shown on the 18th day after implantation. (D) A representative picture of the excised H460/MX20 tumor sizes from different mice is shown on the 18th day after implantation. The treatment was as follows: (a) vehicle (q3d × 6), (b) DOX (1.8 mg/kg, i.p., q3d × 6), (c) telatinib (15 mg/kg, p.o., every 2nd and 3rd day) and (d) DOX (1.8 mg/kg, i.p., q3d × 6) + telatinib (15 mg/kg, p.o., every 2nd and 3rd day, given 1 h before giving DOX). Each column represents the mean determinations and the bars represent SD. Data are means ± SD for 8 animals. At least two independent experiments were carried out using athymic NCR nude mice. The statistical analysis was carried out on day 18. $^{*}P < 0.05$ versus vehicle group; $^{\#}P < 0.05$ versus DOX and telatinib group in (A) and (B), respectively.

with the nitrogen atom of the side chain imidazole ring present in H630 (–NH···N-H630, 2.6 Å). Through site-directed mutagenesis studies, it has been reported that H630 in ABCG2 plays a critical role in the function of ABCG2 [41]. Moreover terminal chlorophenyl ring is involved in hydrophobic interaction with the side chains of the F507, F511 and L633.

### *3.8. Telatinib potentiates the anticancer activity of doxorubicin in ABCG2-overexpressing tumor xenograft nude mouse model*

The parental H460 and MX-selected ABCG2 overexpressing H460/MX-20 xenograft MDR model in athymic nude mice was used to investigate the efficacy of telatinib to reverse the resistance to DOX *in vivo*. Telatinib at 15 mg/kg oral dose was chosen based on our preliminary study where we monitored the tumor efficacy (data not shown) and had no visible toxicity or phenotypic changes in the male athymic NCR nude mice. DOX at 1.8 mg/kg i.p. dose showed appreciable growth retardation in the parental H460 xenografts but not in H460/MX20 xenografts (Fig. 6A–D). The H460/MX20 tumor growth rate recorded over a period of 18 days was significantly slow in the telatinib-DOX combination group compared to vehicle, telatinib alone or DOX alone groups (Fig. 6B). In addition, telatinib in combination with DOX also produced a significant reduction in tumor size and weight (Figs. 6 and 7B). It should be noted that telatinib by itself also significantly decreased the growth rate of H460 and H460/MX20 xenografts. However, there was no significant difference between the effects of telatinib alone or combination on the H460 xenografts (Figs. 6A, C and 7A). DOX with or without telatinib did not produce any apparent toxicity or weight loss (Fig. 7C). Immunohistochemical analysis of the excised tumors showed expression of ABCG2 in H460/MX20 tumors and there was no significant difference in the expression level of the ABCG2 among different groups. Taken together, telatinib did not increase the toxicity; instead it improved the efficacy of DOX in the H460/MX20 xenograft model.

## 4. Discussion

In the current study, we examined the effect of telatinib on ABCG2-mediated drug resistance *in vitro* and *in vivo*. In our cell viability assay, telatinib potentiated the cytotoxicity of ABCG2 substrate anticancer drugs in *ABCG2*-transfected cells and drug selected ABCG2 over-expressing cancer cells. But it had no effect on the parental cells that lack the ABCG2 transporter. However, telatinib had no effect on ABCB1-, ABCC1- and ABCC10-mediated MDR (data not shown). Telatinib itself at the experimentally used concentrations had no significant cytotoxicity on the cell lines used in this study *in vitro*. These observations suggest that telatinib selectively potentiates the cytotoxicity of the ABCG2 substrate anticancer drugs and reverses ABCG2-mediated MDR.

To investigate the mechanism of the reversal of ABCG2-mediated MDR, we analyzed the effect of telatinib on ABCG2-mediated drug transport, ABCG2 expression and its localization *in vitro*. Telatinib increased the accumulation of MX and decreased the efflux rate in cells transfected with *ABCG2*. Furthermore, telatinib did not affect either expression or localization of ABCG2. However, effect of telatinib on localization still needs to be confirmed by more sensitive means. It indicates that increase in

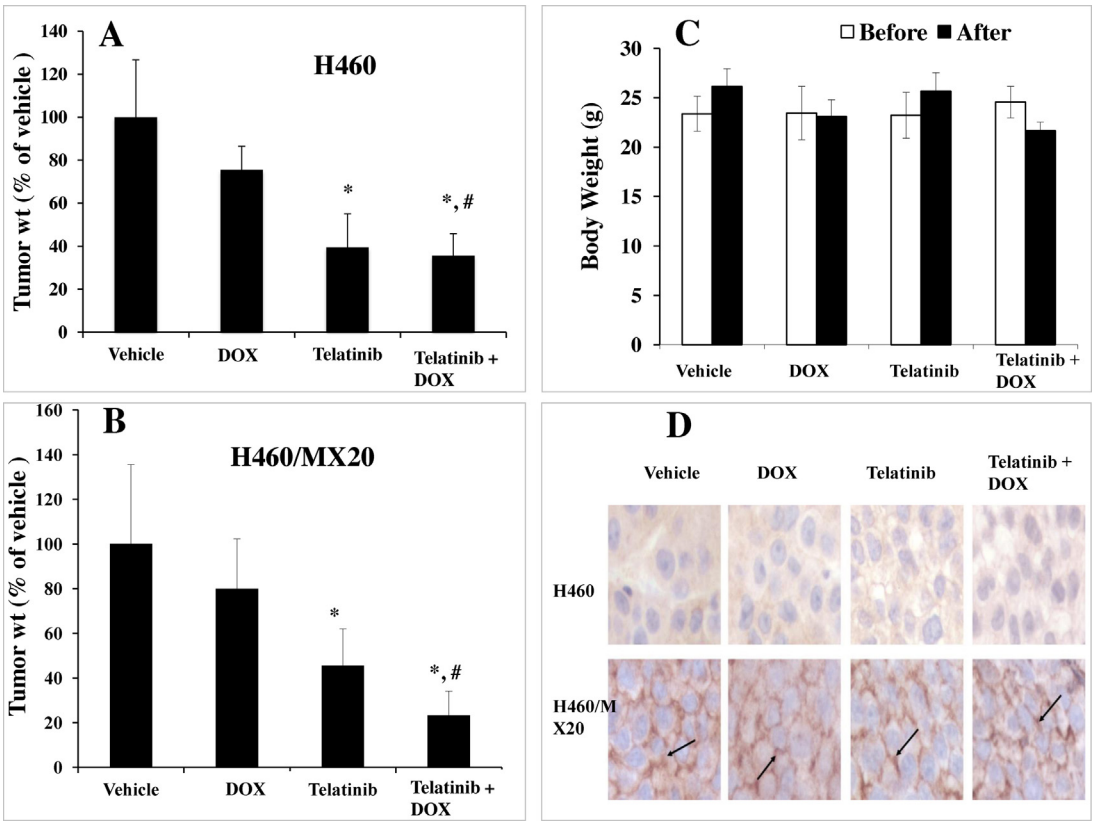


**Fig. 7.** The effect of telatinib on H460 and H460/MX20 tumor xenograft mice. (A) The bar graph represents the mean tumor weight ($n = 8$) of the excised H460 tumor from different mice. (B) The bar graph represents the mean tumor weight ($n = 8$) of the excised H460/MX20 tumor from different mice. (C) Changes in mean body weight before and after treatment for xenograft model are shown in the bar graph. (D) ABCG2 expression analysis by immunohistochemistry in tumor tissues collected from different groups at the end of the xenograft study. There was no ABCG2 expression in the H460 tumors (upper row), while ABCG2 expressed specifically in the cell membrane of H460/MX 20 tumors (lower low, arrows). $^{*}P < 0.05$ versus vehicle group; $^{\#}P < 0.05$ versus DOX and telatinib group in (A) and (B), respectively.

MX levels in the cells expressing ABCG2 is because of inhibition of ABCG2 drug efflux function by telatinib. Some selective ABCG2 inhibitors, such as acrylonitrile derivatives, YHO-13177 and YHO-13351, have been reported to inhibit the function well as expression of ABCG2 [45]. Drugs such as LY294002 (PI3K inhibitor) [46] SGI-1776 (PIM-1 kinase inhibitor) [47] telmisartan and rosiglitazone (PPAR-Y antagonists) [48] were reported to alter the membrane localization of ABCG2 transporter. Telatinib stimulated the ABCG2 ATPase activity in a concentration dependent manner. In addition telatinib effectively reduced the ATP-dependent uptake of [$^3$H]-$E_2$17βG in membrane vesicles obtained from ABCG2-482-R2 without affecting the uptake in the parental HEK293/pcDNA3.1 vesicles. This shows the ability of telatinib to directly interact with the ABCG2 membrane transporter and thereafter inhibiting its transport activity at sub-micromolar concentrations.

However, several other TKIs with ABCB1 and ABCG2 inhibition activity have been shown to be substrates of ABCG2 at low concentration and inhibitors at higher concentration [43,44,49]. In addition, one of the major problems with ABC transporter inhibitors is a severe side effect upon combining with anticancer drugs in clinical trials. FTC, a relatively specific inhibitor of ABCG2, was reported to be neurotoxic in clinical trials [25]. Here we report that telatinib selectively inhibits ABCG2 drug efflux function. Report also suggests that it can be combined with chemotherapeutic drugs without addition of severe side effects. It further indicates that telatinib may be used in combination with other chemotherapeutic drugs.

To identify the binding interactions of the telatinib with ABCG2 transporter, we performed a molecular docking study at highly scored druggable site on homology modeled functionally active dimer form of human ABCG2. Telatinib appears to exhibit the important pharmacophoric features, like hydrophobic groups and/or aromatic ring centers, hydrogen bond acceptor and hydrogen bond donor groups, that have been described critical for binding to ABCG2 and its inhibition [50]. In the absence of co-crystal structure of telatinib-ABCG2, the docking model will form the basis for the future optimization of telatinib to understand the molecular mechanism and to design more potent ABCG2 inhibitors. These favorable binding interactions of telatinib toward ABCG2, support that it may modulate the ABCG2 transporter and its substrates. Recent studies have shown ABCG2 as molecular determinant of side population in various cancer tumors, which is a fraction with high presence of cancer stem cells [18]. This side population with cancer stem cells with ABCG2 expression exhibits drug resistance [24]. Incomplete elimination of the cancer stem cells by chemotherapy can result in tumor relapse. Telatinib in combination with ABCG2 substrate anticancer drugs may lead to complete eradication of cancer stem cells and improved clinical outcome. Further studies are required to examine this phenomenon.

Our H460/MX20 (ABCG2 expressing) xenograft model showed significant resistance to DOX, an ABCG2 substrate and conventional anticancer drug. Telatinib significantly enhanced the anticancer activity of DOX in H460/MX20 xenograft. The positive outcome implies that telatinib can be combined with conventional ABCG2 substrate chemotherapeutic drugs as well as other TKIs that are substrates of ABCG2. Telatinib alone also showed antitumor activity *in vivo* in both H460 and H460/MX20 xenograft model. We believe it could be because of its effect on inhibitory effect on VEGFR. There was no significant difference in the H460 tumor

growth rate in telatinib alone or combination treatment group and DOX showed significant anticancer activity compared to vehicle control group in H460 xenograft. Over all, it suggests that ABCG2 inhibition by telatinib in H460/MX20 xenograft is playing a significant role in synergistic anticancer activity. Additional pharmacokinetic and toxicological studies still required for combination study of telatinib and ABCG2 substrate anticancer drugs. Clinical studies have reported that telatinib is well tolerated up to 1500 mg (bid) with recommended dose of 900 mg bid [31,51]. The recommended dose of 900 mg (bid) gave $C_{max}$ of around 2.5 μM [31,51,52], which is higher than the concentration we used in our *in vitro* and possibly *in vivo* study. Cytochrome-P450 isoforms and UGT1A4 are the major enzymes involved in the metabolism of telatinib with major biotransformation into N-glucuronides form in man [31]. These results indicate that telatinib potentiates the anticancer effect of DOX in H460/MX20 xenograft model at concentrations that are clinically achievable.

In conclusion, our results show that telatinib selectively inhibits ABCG2 and potentiates the ABCG2 substrate anticancer drugs and induce cell cytotoxicity in cells overexpressing ABCG2 *in vitro* and *in vivo* at clinically achievable concentration. These results indicate that telatinib has the potential to be used in combination with conventional ABCG2 substrate anticancer drugs to combat the MDR-mediated by ABCG2. Further clinical studies are required to address this issue.

## Acknowledgements

We thank Dr. Mark F. Rosenberg and Dr. Zsolt Bikadi (Manchester Interdisciplinary Biocentre, 131 Princess Street, University of Manchester, Manchester, M1 7DN, UK) for providing coordinates of ABCG2 homology model. We are thankful to Drs. Susan E. Bates and Robert W. Robey (NCI, NIH) for HEK293/pcDNA3.1 (parental), ABCG2-482-R2, ABCG2-482-G2, ABCG2-482-T7, H460, H460/MX20, S1, S1-M1-80 cell lines and FTC. We also thank Dr. Suresh Ambudkar for providing HEK/ABCC1 cell line.

## References

[1] Gottesman MM. Mechanisms of cancer drug resistance. Annu Rev Med 2002;53:615–27.
[2] Deeley RG, Westlake C, Cole SP. Transmembrane transport of endo- and xenobiotics by mammalian ATP-binding cassette multidrug resistance proteins. Physiol Rev 2006;86:849–99.
[3] Gottesman MM, Fojo T, Bates SE. Multidrug resistance in cancer: role of ATP-dependent transporters. Nat Rev Cancer 2002;2:48–58.
[4] Dean M. The human ATP-binding cassette (ABC) transporter superfamily. Genome Res 2001;11:1156–66.
[5] Gottesman MM, Ambudkar SV. Overview ABC transporters and human disease. J Bioenerg Biomembr 2001;33:453–8.
[6] Gillet JP, Efferth T, Remacle J. Chemotherapy-induced resistance by ATP-binding cassette transporter genes. Biochim Biophys Acta 2007;1775:237–62.
[7] Loscher W, Potschka H. Drug resistance in brain diseases and the role of drug efflux transporters. Nat Rev Neurosci 2005;6:591–602.
[8] Szakacs G, Varadi A, Ozvegy-Laczka C, Sarkadi B. The role of ABC transporters in drug absorption, distribution, metabolism, excretion and toxicity (ADME-Tox). Drug Discov Today 2008;13:379–93.
[9] Robey RW, Polgar O, Deeken J, To KW, Bates SE. ABCG2: determining its relevance in clinical drug resistance. Cancer Metastasis Rev 2007;26:39–57.
[10] Tiwari AK, Sodani K, Dai CL, Ashby Jr CR, Chen ZS. Revisiting the ABCs of multidrug resistance in cancer chemotherapy. Curr Pharm Biotechnol 2011;12:570–94.
[11] Robey RW, Ierano C, Zhan Z, Bates SE. The challenge of exploiting ABCG2 in the clinic. Curr Pharm Biotechnol 2011;12:595–608.
[12] Natarajan K, Xie Y, Baer MR, Ross DD. Role of breast cancer resistance protein (BCRP/ABCG2) in cancer drug resistance. Biochem Pharmacol 2012;83:1084–103.
[13] Steinbach D, Sell W, Voigt A, Hermann J, Zintl F, Sauerbrey A. BCRP gene expression is associated with a poor response to remission induction therapy in childhood acute myeloid leukemia. Leukemia 2002;16:1443–7.
[14] van den Heuvel-Eibrink MM, Wiemer EA, Prins A, Meijerink JP, Vossebeld PJ, van der Holt B, et al. Increased expression of the breast cancer resistance protein (BCRP) in relapsed or refractory acute myeloid leukemia (AML). Leukemia 2002;16:833–9.
[15] Candeil L, Gourdier I, Peyron D, Vezzio N, Copois V, Bibeau F, et al. ABCG2 overexpression in colon cancer cells resistant to SN38 and in irinotecan-treated metastases. Int J Cancer 2004;109:848–54.
[16] Diestra JE, Scheffer GL, Catala I, Maliepaard M, Schellens JH, Scheper RJ, et al. Frequent expression of the multi-drug resistance-associated protein BCRP/MXR/ABCP/ABCG2 in human tumours detected by the BXP-21 monoclonal antibody in paraffin-embedded material. J Pathol 2002;198:213–9.
[17] Galimberti S, Guerrini F, Palumbo GA, Consoli U, Fazzi R, Morabito F, et al. Evaluation of BCRP and MDR-1 co-expression by quantitative molecular assessment in AML patients. Leuk Res 2004;28:367–72.
[18] Zhou S, Schuetz JD, Bunting KD, Colapietro AM, Sampath J, Morris JJ, et al. The ABC transporter Bcrp1/ABCG2 is expressed in a wide variety of stem cells and is a molecular determinant of the side-population phenotype. Nat Med 2001;7:1028–34.
[19] Abbott BL. ABCG2 (BCRP) expression in normal and malignant hematopoietic cells. Hematol Oncol 2003;21:115–30.
[20] Hirschmann-Jax C, Foster AE, Wulf GG, Nuchtern JG, Jax TW, Gobel U, et al. A distinct "side population" of cells with high drug efflux capacity in human tumor cells. Proc Natl Acad Sci U S A 2004;101:14228–33.
[21] Visvader JE, Lindeman GJ. Cancer stem cells in solid tumours: accumulating evidence and unresolved questions. Nat Rev Cancer 2008;8:755–68.
[22] Bleau AM, Hambardzumyan D, Ozawa T, Fomchenko EI, Huse JT, Brennan CW, et al. PTEN/PI3K/Akt pathway regulates the side population phenotype and ABCG2 activity in glioma tumor stem-like cells. Cell Stem Cell 2009;4:226–35.
[23] Reya T, Morrison SJ, Clarke MF, Weissman IL. Stem cells, cancer, and cancer stem cells. Nature 2001;414:105–11.
[24] Dean M, Fojo T, Bates S. Tumour stem cells and drug resistance. Nat Rev Cancer 2005;5:275–84.
[25] Rabindran SK, He H, Singh M, Brown E, Collins KI, Annable T, et al. Reversal of a novel multidrug resistance mechanism in human colon carcinoma cells by fumitremorgin C. Cancer Res 1998;58:5850–8.
[26] Dai CL, Tiwari AK, Wu CP, Su Xd, Wang SR, Liu Dg. et al. Lapatinib (Tykerb, GW572016) reverses multidrug resistance in cancer cells by inhibiting the activity of ATP-binding cassette subfamily B member 1 and G member 2. Cancer Res 2008;68:7905–14.
[27] Shi Z, Peng XX, Kim IW, Shukla S, Si QS, Robey RW, et al. Erlotinib (Tarceva, OSI-774) antagonizes ATP-binding cassette subfamily B member 1 and ATP-binding cassette subfamily G member 2 mediated drug resistance. Cancer Res 2007;67:11012–20.
[28] Sodani K, Tiwari AK, Singh S, Patel A, Xiao ZJ, Chen JJ, et al. GW583340 and GW2974, human EGFR and HER-2 inhibitors, reverse ABCG2- and ABCB1-mediated drug resistance. Biochem Pharmacol 2012;83:1613–22.
[29] Tiwari AK, Sodani K, Wang SR, Kuang YH, Ashby Jr CR, Chen X, et al. Nilotinib (AMN107, Tasigna) reverses multidrug resistance by inhibiting the activity of the ABCB1/Pgp and ABCG2/BCRP/MXR transporters. Biochem Pharmacol 2009;78:153–61.
[30] Tiwari AK, Sodani K, Dai CL, Abuznait AH, Singh S, Xiao ZJ, et al. Nilotinib potentiates anticancer drug sensitivity in murine ABCB1-, ABCG2-, and ABCC10-multidrug resistance xenograft models. Cancer Lett 2013;328:307–17.
[31] Eskens FA, Steeghs N, Verweij J, Bloem JL, Christensen O, van Doorn L, et al. Phase I dose escalation study of telatinib, a tyrosine kinase inhibitor of vascular endothelial growth factor receptor 2 and 3, platelet-derived growth factor receptor beta, and c-Kit, in patients with advanced or metastatic solid tumors. J Clin Oncol 2009;27:4169–76.
[32] Sodani K, Patel A, Kathawala RJ, Chen ZS. Multidrug resistance associated proteins in multidrug resistance. Chin J Cancer 2012;31:58–72.
[33] Bliss CI. The calculation of the dosage–mortality curve. Ann Appl Biol 1935;22:134–67.
[34] Sarkadi B, Price EM, Boucher RC, Germann UA, Scarborough GA. Expression of the human multidrug resistance cDNA in insect cells generates a high activity drug-stimulated membrane ATPase. J Biol Chem 1992;267:4854–8.
[35] Chen ZS, Robey RW, Belinsky MG, Shchaveleva I, Ren XQ, Sugimoto Y, et al. Transport of methotrexate, methotrexate polyglutamates, and 17beta-estradiol 17-(beta-D-glucuronide) by ABCG2: effects of acquired mutations at R482 on methotrexate transport. Cancer Res 2003;63:4048–54.
[36] Aller SG, Yu J, Ward A, Weng Y, Chittaboina S, Zhuo R, et al. Structure of P-glycoprotein reveals a molecular basis for poly-specific drug binding. Science 2009;323:1718–22.
[37] Rosenberg MF, Bikadi Z, Chan J, Liu X, Ni Z, Cai X, et al. The human breast cancer resistance protein (BCRP/ABCG2) shows conformational changes with mitoxantrone. Structure 2010;18:482–93.
[38] Hazai E, Bikadi Z. Homology modeling of breast cancer resistance protein (ABCG2). J Struct Biol 2008;162:63–74.
[39] Robey RW, Honjo Y, Morisaki K, Nadjem TA, Runge S, Risbood M, et al. Mutations at amino-acid 482 in the ABCG2 gene affect substrate and antagonist specificity. Br J Cancer 2003;89:1971–8.
[40] Mitomo H, Kato R, Ito A, Kasamatsu S, Ikegami Y, Kii I, et al. A functional study on polymorphism of the ATP-binding cassette transporter ABCG2: critical role of arginine-482 in methotrexate transport. Biochem J 2003;373:767–74.
[41] Miwa M, Tsukahara S, Ishikawa E, Asada S, Imai Y, Sugimoto Y. Single amino acid substitutions in the transmembrane domains of breast cancer resistance protein (BCRP) alter cross resistance patterns in transfectants. Int J Cancer 2003;107:757–63.

[42] Alqawi O, Bates S, Georges E. Arginine482 to threonine mutation in the breast cancer resistance protein ABCG2 inhibits rhodamine 123 transport while increasing binding. Biochem J 2004;382:711–6.
[43] Hegedus C, Truta-Feles K, Antalffy G, Varady G, Nemet K, Ozvegy-Laczka C, et al. Interaction of the EGFR inhibitors gefitinib, vandetanib, pelitinib and neratinib with the ABCG2 multidrug transporter: implications for the emergence and reversal of cancer drug resistance. Biochem Pharmacol 2012;84:260–7.
[44] Hegedűs C, Özvegy-Laczka C, Apáti Á, Magócsi M, Német K, Őrfi L, et al. Interaction of nilotinib, dasatinib and bosutinib with ABCB1 and ABCG2: implications for altered anti-cancer effects and pharmacological properties. Br J Pharmacol 2009;158:1153–64.
[45] Yamazaki R, Nishiyama Y, Furuta T, Hatano H, Igarashi Y, Asakawa N, et al. Novel acrylonitrile derivatives, YHO-13177 and YHO-13351, reverse BCRP/ABCG2-mediated drug resistance in vitro and in vivo. Mol Cancer Ther 2011;10:1252–63.
[46] Goler-Baron V, Sladkevich I, Assaraf YG. Inhibition of the PI3K–Akt signaling pathway disrupts ABCG2-rich extracellular vesicles and overcomes multidrug resistance in breast cancer cells. Biochem Pharmacol 2012;83:1340–8.
[47] Natarajan K, Bhullar J, Shukla S, Burcu M, Chen ZS, Ambudkar SV, et al. The Pim kinase inhibitor SGI-1776 decreases cell surface expression of P-glycoprotein (ABCB1) and breast cancer resistance protein (ABCG2) and drug transport by Pim-1-dependent and -independent mechanisms. Biochem Pharmacol 2013;85:514–24.
[48] To KK, Tomlinson B. Targeting the ABCG2-overexpressing multidrug resistant (MDR) cancer cells by PPARgamma agonists. Br J Pharmacol 2013;170:1137–51.
[49] Brozik A, Hegedus C, Erdei Z, Hegedus T, Ozvegy-Laczka C, Szakacs G, et al. Tyrosine kinase inhibitors as modulators of ATP binding cassette multidrug transporters: substrates, chemosensitizers or inducers of acquired multidrug resistance. Expert Opin Drug Metab Toxicol 2011;7:623–42.
[50] Ecker G, Chiba P. Transporters as drug carriers: structure, function, substrates. Weinheim: Wiley-VCH; 2009.
[51] Strumberg D, Schultheis B, Adamietz IA, Christensen O, Buechert M, Kraetzschmar J, et al. Phase I dose escalation study of telatinib (BAY 57-9352) in patients with advanced solid tumours. Br J Cancer 2008;99:1579–85.
[52] Mross K, Frost A, Scheulen ME, Krauss J, Strumberg D, Schultheiss B, et al. Phase I study of telatinib (BAY 57-9352): analysis of safety, pharmacokinetics, tumor efficacy, and biomarkers in patients with colorectal cancer. Vasc Cell 2011;3:16.